IAC-16-C1.4.5

OPTIMISATION OF LOW-THRUST AND HYBRID EARTH-MOON TRANSFERS

Nicola Sullo
School of Engineering, University of Glasgow, Glasgow, United Kingdom, n.sullo.1@research.gla.ac.uk

Priscilla A. de Sousa-Silva
Instituto Tecnológico de Aeronáutica (ITA), Brazil, priandss@ita.br

Maisa O. Terra
Instituto Tecnológico de Aeronáutica (ITA), Brazil, maisa@ita.br

Matteo Ceriotti
School of Engineering, University of Glasgow, Glasgow, United Kingdom, matteo.ceriotti@glasgow.ac.uk

This paper presents an optimization procedure to generate fast and low-Δv Earth-Moon transfer trajectories, by exploiting the multi-body dynamics of the Sun-Earth-Moon system. Ideal (first-guess) trajectories are generated at first, using two coupled planar circular restricted three-body problems, one representing the Earth-Moon system, and one representing the Sun-Earth. The trajectories consist of a first ballistic arc in the Sun-Earth system, and a second ballistic arc in the Earth-Moon system. The two are connected at a patching point at one end (with an instantaneous Δv), and they are bounded at Earth and Moon respectively at the other end. Families of these trajectories are found by means of an evolutionary optimization method. Subsequently, they are used as first-guess for solving an optimal control problem, in which the full three-dimensional 4-body problem is introduced and the patching point is set free. The objective of the optimisation is to reduce the total Δv, and the time of flight, together with introducing the constraints on the transfer boundary conditions and of the considered propulsion technology. Sets of different optimal trajectories are presented, which represents trade-off options between Δv and time of flight. These optimal transfers include conventional solar-electric low-thrust and hybrid chemical/solar-electric high/low-thrust, envisaging future spacecraft that can carry both systems. A final comparison is made between the optimal transfers found and only chemical high-thrust optimal solutions retrieved from literature.

I. INTRODUCTION

Missions to the Moon have acquired more interest recently. In fact, in addition to scientific reasons, the Moon is an appealing destination as it can be a source of raw materials and even of energy for the human use, and as an intermediate gateway for transferring to other, farther destinations in the solar system.[1–3] In the last decades, numerous studies have been carried out in order to design transfer strategies to reach the Moon efficiently. Indeed space missions generally require a minimised fuel mass consumption, in order to both make feasible the mission itself and reduce the overall costs. At the same time the necessity often arises to reduce the total time of flight. This can be due, for example, to the need to reduce the radiation doses of a particular payload, or human crew, and reduce the operation costs. Recent strategies to design fast and low-energy Earth-Moon transfers make use of multi-body dynamical models in order to exploit their high nonlinearities, which are regarded only as unwanted perturbations in the simplest Keplerian two-body dynamics. In this paper, an optimisation strategy is proposed to design optimal transfers to the Moon, making use of a 4-body dynamical model to compute efficient transfer solutions, both in terms of fuel mass consumption and time of flight. The optimisation process starts from first guess trajectories, generated in a coupled 3-body dynamical system and bounded both at the Earth and the Moon.[4,5] These initial guess trajectories are made up of two ballistic arcs connected at a patching point, with patching Δv of the order of a hundred m/s and transfer time of about ten days. These first guess solutions guarantee ballistic capture at the Moon, however they just pass by the perigee at the Earth. Therefore the work described here also add the optimisation of an orbit-raising phase, which is required in order to escape from a parking orbit around the Earth and inject into the main transfer trajectory to the Moon. Starting from the first-guess solutions, the optimisation process produces sets of optimal Earth-Moon transfer trajectories each exploiting a different propulsion technology, such as conventional solar-electric low-thrust and hybrid chemical/solar-electric high/low-thrust. These solutions represent trade-off options – between the time of flight and the fuel consumption – for a more convenient design of an Earth-Moon transfer, according to specific mission requirements and

constraints. The paper is organized as follows. In section II the adopted mathematical models are described and they regard both the dynamics and the reference systems used. In section III the process for the generation of the first guess trajectories is introduced, a set of initial guesses is selected and an explanation is provided on how these starting solutions have been used in the optimisation process. The optimal control problem (OCP) setup and resolution strategy is explained in detail in section IV. In section V a full summary of the results is provided and the best solutions obtained – both for low and hybrid thrust Earth-Moon transfers – are illustrated, discussed and compared with only chemical high-thrust optimal solutions retrieved from literature. The conclusions are finally given in section VI.

II. MATHEMATICAL MODELS

An explanation of the dynamical models adopted, as well as the reference frames and coordinates system used, is necessary for a correct understanding of the optimal control problems subsequently stated and the overall optimisation framework set up for the Earth-Moon transfers. The three-dimensional bi-circular restricted 4-body problem (BCR4BP) dynamics has been used in the optimisation of the main Earth-Moon transfers. Two coupled circular restricted 3-body problem (CR3BP) dynamics – relative to the Sun-Earth and Earth-Moon systems – have been used in the generation of the initial guesses required for the solution of the trajectory optimisation problem related to the main Earth-Moon transfer. Inertial and synodic reference frames have been used in the current studies and they are illustrated in detail in the following subsections, together with the aforementioned dynamics models.

II.I Reference frames and coordinates system

The Sun-centred inertial reference frame has been used in the transcription of the optimal control problem, while two further frames, the Sun-Earth synodic and the Earth-Moon synodic, have been used in the process of generation of the initial guesses of the optimal Earth-Moon transfers. Specifically, the Sun-centred inertial frame has the X-axis pointing towards the γ-point and the X-Y plane coinciding with the plane of the ecliptic, as shown in Figure 1.

The synodic frames are associated to a CR3BP dynamical system where the gravitational field is generated by two main attraction bodies, also defined as primaries (m_1 the larger and m_2 the smaller), rotating at constant angular velocity and describing circular orbits around their barycentre. The third body (e.g.: a spacecraft) has a negligible mass and is subjected to the primaries gravitational attraction forces.[6,7]

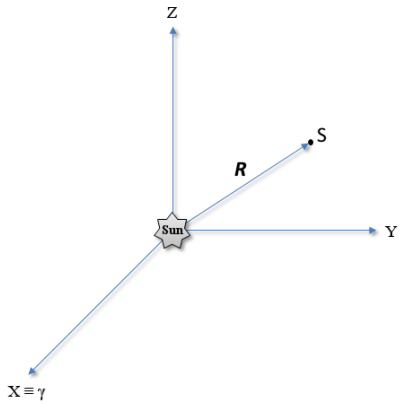

Figure 1. Sun-centred inertial reference frame. The X-axis points towards the vernal equinox point, the Z-axis points towards the north ecliptic pole and the Y-axis completes the right-handed triad.

The synodic frames have the x-axis passing by the primaries (with direction going from the larger to the smaller), z-axis having the same direction and sense of the angular velocity vector of rotation of the primaries, y-axis on the plane of rotation of the primaries, as shown in Figure 2. The origin of the reference system is placed in the barycentre of the primaries masses. Clearly, the Sun-Earth synodic frame has the Sun as main attraction body and the Earth as secondary attraction body; on the same fashion, the Earth-Moon synodic frame has the Earth as main attraction body and the Moon as secondary attraction body. If non-dimensional units are considered and the distance between the primaries is considered as a length-unit, the position of the primaries can be expressed as function of the mass ratio $\mu = \frac{m_2}{m_1 + m_2}$, as shown in Figure 2.

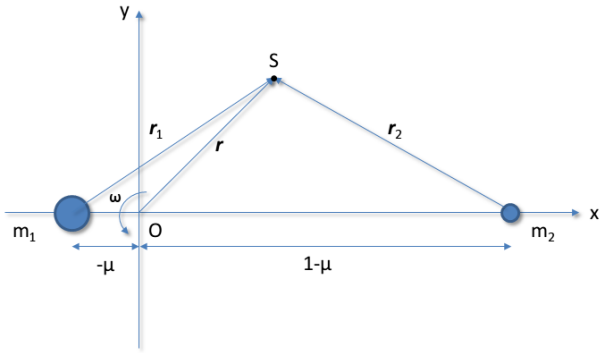

Figure 2. Synodic reference frame. The origin O of the reference frame is placed in the barycentre of the primaries. The x-axis passes by the primaries with direction going from the larger to the smaller, the z-axis has the same direction and sense of the angular velocity vector of the system, the y-axis completes the right-handed triad.

The coordinates system used is the Cartesian one, adopted both in the inertial and synodic systems. For reason of clarity, the Cartesian coordinates related to the synodic system are expressed in lowercase letters while, conversely, for the inertial system they are expressed in uppercase letters. Therefore, the state of a generic point S in the space can be expressed as:

$$ {}^{I}\boldsymbol{y}_S = \left[\boldsymbol{R} \quad \boldsymbol{V}\right]^T = \left[R_x \quad R_y \quad R_z \quad V_x \quad V_y \quad V_z\right]^T \quad (1) $$

in the inertial reference frame, and as

$$ {}^{S}\boldsymbol{y}_S = \left[\boldsymbol{r} \quad \boldsymbol{v}\right]^T = \left[r_x \quad r_y \quad r_z \quad v_x \quad v_y \quad v_z\right]^T \quad (2) $$

in the synodic reference frame.

Dimensionless units have been used in the dynamics equations and in the optimal control problem statements. Two different scalings have been adopted, a first one for the Sun-centred inertial and Sun-Earth synodic frames, a second one for the Earth-Moon synodic frame. In the first scaling the average distance between the Sun and the Earth has been considered as length-unit and the solar year as time-unit. In the second scaling, instead, the average distance between the Earth and the Moon has been considered as length-unit and the synodic month as time-unit. In addition, when considering the spacecraft's mass variation in the OCP solution, the mass is normalised to the initial spacecraft mass.

II.II Dynamical models

CR3BP

The circular-restricted 3-body problem dynamics, as already mentioned, has been used in the procedure to generate the initial guesses, required for the subsequent optimisation of the Earth-Moon transfers. Although well-known in literature[6,7], the CR3BP dynamics equations are below stated in (3), for reason of clarity in the exposition:

$$ \begin{cases} \dot{x} = v_x \\ \dot{y} = v_y \\ \dot{z} = v_z \\ \dot{v}_x = 2v_y + x - \dfrac{1-\mu}{r_1^3}(x+\mu) - \dfrac{\mu}{r_2^3}(x-1+\mu) \\ \dot{v}_y = -2v_x + y - \left(\dfrac{1-\mu}{r_1^3} + \dfrac{\mu}{r_2^3}\right) y \\ \dot{v}_z = -\left(\dfrac{1-\mu}{r_1^3} + \dfrac{\mu}{r_2^3}\right) z \end{cases} \quad (3) $$

In (3) dimensionless units have been considered, according to the scaling previously described.

Coupled-CR3BP configuration

The coupled 3-body dynamics[4,5] is a simplified representation of the more complex 4-body dynamical system and made-up by coupling together two different CR3BP dynamical systems. This simplified representation of the 4-body dynamics model has the important advantage to allow making use of the dynamical peculiarities of each CR3BP system separately. Therefore transfer trajectories can be computed in each 3-body system and properly patched in order to get an overall transfer in the (simplified) 4-body dynamical system. An illustrative representation of the coupled 3-body dynamics configuration is provided in Figure 3, for the case of the Sun-Earth-Moon system.

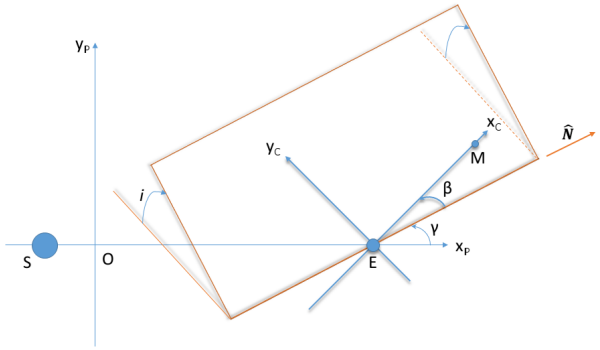

Figure 3. Coupled-CR3BP configuration.

As shown in Figure 3, the "parent" system corresponds to the Sun-Earth CR3BP (x_P,y_P,z_P), the "child" system instead corresponds to the Earth-Moon CR3BP (x_C,y_C,z_C), with origin in the Earth. The child system is tilted by $i = 5.145°$ with respect to the plane ($x_P O y_P$). The intersection between the planes ($x_P O y_P$) and ($x_C E y_C$) identifies the line of nodes with direction $\hat{N}$ fixed in an inertial reference frame. Both the parent and the child systems rotate around their z-axis with their respective (constant) angular velocity. The mutual orientation of each reference frame with respect to the other is identified by the angles γ and β. γ denotes the angular position of the x-axis of the parent system with respect to the nodes line; β instead identifies the angular position of the x-axis of the child system with respect to the nodes line. It has to be noted that the patching between the trajectories computed in the parent and the child system takes place in a so called "patching" area, defined as a spherical-ring region around the Moon, with inner radius of 70000 km and outer radius of 90000 km. For further details the reader can refer to [4].

BCR4BP

The BCR4BP dynamical model uses three main attraction bodies as primaries and specifically, for the current case of study, these are the Sun, the Earth and the Moon. The reference frame used is the Sun-centred inertial. The Earth describes, on the ecliptic plane, a circular orbit around the Sun with radius equal to 1 AU. The Moon describes a circular orbit around the Earth, with radius equal to the mean Earth-Moon distance: this orbit takes place on a plane tilted by $i = 5.145°$ with respect to the ecliptic. The dynamics equations of the BCR4BP in the inertial frame are provided in equation (4) below, in which the overall acceleration is expressed by the sum of the gravitational accelerations $\boldsymbol{a}_\odot$, $\boldsymbol{a}_\oplus$, $\boldsymbol{a}_M$ due respectively to the Sun, Earth and Moon:

$$\ddot{\boldsymbol{R}} = \underbrace{-\mu_\odot \frac{\boldsymbol{R}}{\|\boldsymbol{R}\|^3}}_{\boldsymbol{a}_\odot} \underbrace{-\mu_\oplus \frac{(\boldsymbol{R}-\boldsymbol{R}_\oplus)}{\|\boldsymbol{R}-\boldsymbol{R}_\oplus\|^3}}_{\boldsymbol{a}_\oplus} \underbrace{-\mu_M \frac{(\boldsymbol{R}-\boldsymbol{R}_M)}{\|\boldsymbol{R}-\boldsymbol{R}_M\|^3}}_{\boldsymbol{a}_M} \tag{4}$$

where $\mu_\odot$, $\mu_\oplus$ and μ_M are respectively the gravitational parameters of the Sun, the Earth and the Moon; $\boldsymbol{R}_\oplus$ and $\boldsymbol{R}_M$ respectively the positions, in the inertial frame, of the Earth and the Moon.

III. INITIAL GUESSES

The initial guess trajectories - used as a starting solution in the subsequent optimisation process - are computed in the coupled-CR3BP dynamical model. They consist of a first ballistic arc in the Sun-Earth system, and a second ballistic arc in the Earth-Moon system. The two arcs are connected at a patching point on the line of the nodes at one end (with an impulsive Δv), and they are bounded at Earth and Moon respectively at the other end. Families of these trajectories are found by means of the NSGA-II software, with patching Δv of the order of a hundred m/s and transfer time of about 10 days. The Earth-Moon trajectories end up into a Moon capture phase, lasting around 169 days for each initial guess solution. For further details, the reader is referred to [5] for a comprehensive explanation of the initial guesses generation procedure.
Specifically, three different initial guesses have been selected, belonging to three distinct families characterised by a different altitude at the Earth's closest approaching point. A summary of the characteristics of the three initial guesses, selected and used in the subsequent optimisations, is provided in Table 1.

Table 1. Main characteristics of the selected initial guess for the Earth-Moon transfers

IG #	h_{ECAP} [km]	h_{MCAP} [km]	Δv_P [m/s]	t_{0f} [days]	t_{CAP} [days]
1	100000	96.28	78.11	12.23	168.82
2	60000	96.28	166.82	11.73	169
3	35786	96.28	274.30	11.11	169.67

In Table 1, h_{ECAP} denotes the altitude at the Earth's closest approaching point, h_{MCAP} the altitude at the Moon's closest approaching point, Δv_P the impulsive Δv at the patching point, t_{0f} the time of flight of the transfer, t_{CAP} the time of capture around the Moon.
In order to conveniently make use of the selected initial guess trajectories (as starting point to compute optimal transfers in the 4-body dynamics), it has been necessary to provide them with the discrepancy acceleration with respect to the BCR4BP dynamical model. This acceleration $\boldsymbol{a}_d$ is retrieved by considering it as an excess acceleration with respect to the 4-body dynamics equation of motion, as stated by:

$$\boldsymbol{a}_d = \frac{d^2\boldsymbol{R}}{dt^2} - \boldsymbol{a}_\odot - \boldsymbol{a}_\oplus - \boldsymbol{a}_M \tag{5}$$

In this way the initial guess solutions have been turned into feasible trajectories in the 4-body dynamics, thus making easier for the optimiser to converge to an optimal solution. In fact the optimiser only has to improve the starting solution provided, rather than firstly finding a feasible and next an optimal solution. In Figure 4, Figure 5 and Figure 6 the plots of the magnitude of $\boldsymbol{a}_d$ are shown, respectively for the IG1, IG2 and IG3. A discontinuity in the discrepancy acceleration appears in each of these three plots, taking place at the patching point location.

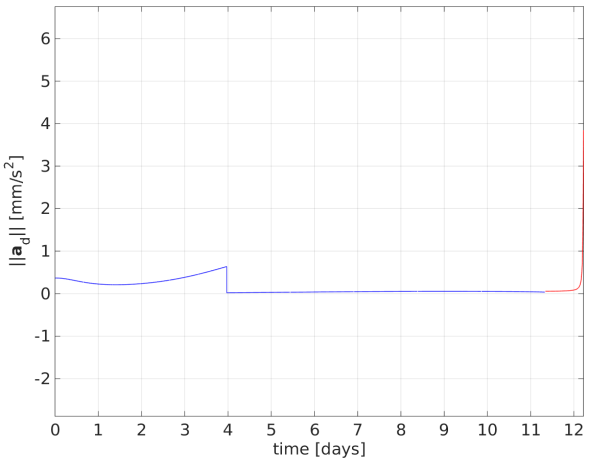

Figure 4. Magnitude of the discrepancy acceleration for the IG1 solution.

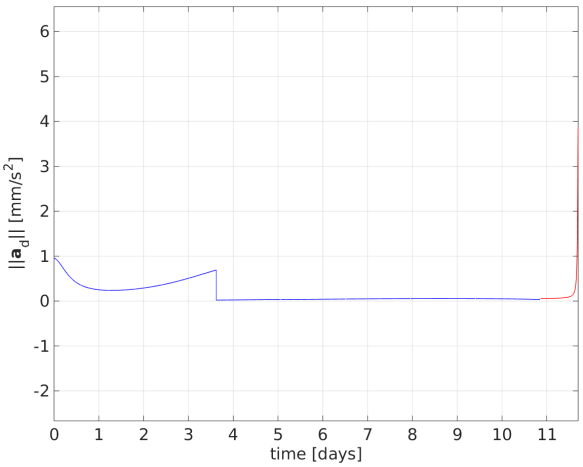

Figure 5. Magnitude of the discrepancy acceleration for the IG2 solution.

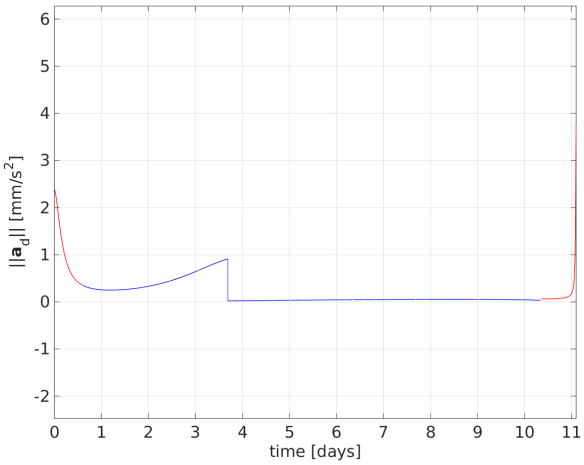

Figure 6. Magnitude of the discrepancy acceleration for the IG3 solution.

As shown in Figure 4, Figure 5 and Figure 6, a peak acceleration of around 4 mm/s^2 takes place in the last part of the transfer, in the proximity of the Moon; in the case of the third initial guess, another peak of about 2.5 mm/s^2 appears also in the initial part of the transfer, close to the departure from the Earth (as shown in Figure 6). The authors believe that these peak accelerations do not reflect a real physical behaviour, but they are due to numerical errors in computing the discrepancy acceleration, coming from the choice of the reference system (Sun-centred inertial) adopted in the BCR4BP model. To ease the convergence in the later optimisation, it has been necessary to neglect the last trajectory portion for all the initial guesses and also the initial part in third initial guess, where the peak accelerations appear. The criterion for removing these trajectory portions has been based on trial and error tests. The removed final parts of the initial guess transfers are next used by patching them with the optimal 4-body transfer.

IV. OPTIMAL CONTROL PROBLEM SETUP AND RESOLUTION STRATEGY

As previously mentioned, the problem of computing full and optimal Earth-Moon transfers has been split in two parts, due to the complexity of the overall trajectory optimisation problem. These two parts consist in the main Earth-Moon transfer – ending in a ballistic capture at the Moon – and in the escape trajectory from a departing Earth orbit. In fact different constraints, dynamics and objective functions – as well as numerical solution approaches – have been required to compute optimal solutions for these two sub-problems and, for these reasons, a comprehensive solution of the overall transfer problem would have been hard to be computed in only a single optimisation.

Before describing in detail the numerical resolution approaches used in the computation of the two optimal transfer sub-problems, it should be noted that the escape trajectory from the Earth is the part of the overall Earth-Moon transfer that requires more fuel mass consumption, as shown later in detail in section V. Because of the necessity to find convenient solutions in terms of transfer time while reducing at the same time the costs in terms of fuel mass required, solutions for the escape transfer from the Earth have been computed both for a solar-electric low-thrust and a chemical high-thrust propulsion system. In this way it has been possible to compute sets of trade-off options – between fuel mass consumption and time of flight – which also involve hybrid-thrust transfer solutions. In fact, a purely solar-electric low-thrust minimum-time-of-flight solution guarantees low fuel mass consumptions (due to the higher specific impulse of a solar-electric thruster) together with keeping to the minimum the transfer time required for escaping from the Earth. On another hand, a chemical high-thrust minimum-fuel-consumption solution guarantees fast escape transfers from the Earth while still keeping the fuel-mass consumption bounded within the fuel budget assigned a priori for the mission.

As already mentioned, the end of the Earth-Moon transfer is finally patched with the trajectory relative to the capture phase around the Moon. This part is computed as part of the initial guess in the Earth-Moon system, and not re-optimised here.

In the remainder of this section, the optimal control problem setup and the resolution strategies are shown, firstly for the main Earth-Moon transfer, then for the escape trajectory from the Earth.

IV.I. Earth-Moon transfer

The main Earth-Moon transfer takes place between the end-points relative to the initial guess solution. A direct transcription pseudo-spectral based method has been employed to transform the time-continuous

optimal control problem into a nonlinear programming (NLP) problem, which is next solved by means of a sequential quadratic programming (SQP) algorithm. The authors made use of *GPOPS-II*[8] software – which involves direct transcription and pseudo-spectral method to transform the time-continuous OCP into a NLP problem – and *SNOPT*[9], a software package for solving large-scale nonlinear optimisation problems by means of a SQP algorithm implementation. Automatic differentiation has also been used in order to improve the performance of the SQP algorithm and its convergence to an optimal solution. The *AdiGator*[10] software has been used to generate the derivatives of the objective function and the nonlinear constraints, required by the sequential-quadratic algorithm.

Before stating the optimal control problem, it is firstly necessary to remark that the final optimal solution for the low-thrust Earth-Moon transfer has been obtained after multiple subsequent steps, starting from the solution of the constant-mass problem with a high value of the maximum acceleration $a_{\max}$ (that can be provided by the low-thrust propulsion system). This has been necessary because of the relatively high values of the discrepancy acceleration with respect to the nominal value of the maximum low-thrust acceleration considered for the final solution ($\bar{a}_{\max} = 0.3$ mm/s^2). The departing values of $a_{\max}$ have been chosen empirically, in order to make the optimiser to easily converge to an optimal solution. Then, a continuation process has been employed in which subsequent optimisations have been performed with the aim to find, at each step, an optimal transfer solution with a lower value of $a_{\max}$, respect to the one of the solution at the previous step used as initial guess. At the end of the continuation process an optimal low-thrust constant-mass transfer is eventually found with $a_{\max} = \bar{a}_{\max}$. The step-length (in terms of $\Delta a_{\max}$) at each iteration of the continuation process has been heuristically chosen, in order to always ensure convergence to an optimal solution. Lastly, the constant-mass solution is directly used as initial guess to solve the optimal control problem with variable spacecraft mass and maximum thrust value equal to the nominal one that can be provided by the low-thrust system: $T_{\max} = \bar{T}_{\max} = 0.3$ N.

The starting OCP, defined as $\mathcal{P}_1$, can be stated as the problem to find the optimal control $\boldsymbol{u} = \boldsymbol{u}(t)$ which minimise the objective function

$$J = \int_{t_0}^{t_f} \boldsymbol{u}^T \boldsymbol{u}\, dt \tag{6}$$

subjected to the dynamics and the constraint conditions below explained. The dynamics is the one relative to the BCR4BP with constant spacecraft mass

$$\dot{\boldsymbol{y}} = \boldsymbol{f}\left(\boldsymbol{y}(t), \boldsymbol{u}(t), \boldsymbol{p}, t\right) \tag{7}$$

$$= \begin{cases} \dot{\boldsymbol{R}} = \boldsymbol{V} \\ \dot{\boldsymbol{V}} = -\mu_{\odot} \dfrac{\boldsymbol{R}}{\|\boldsymbol{R}\|^3} - \mu_{\oplus} \dfrac{(\boldsymbol{R} - \boldsymbol{R}_{\oplus})}{\|\boldsymbol{R} - \boldsymbol{R}_{\oplus}\|^3} - \mu_M \dfrac{(\boldsymbol{R} - \boldsymbol{R}_M)}{\|\boldsymbol{R} - \boldsymbol{R}_M\|^3} + a_{\max} \boldsymbol{u} \end{cases}$$

in which $\boldsymbol{p}$ is the vector of the constant parameters involved in the optimal problem formulation, $\boldsymbol{u} = \begin{bmatrix} u_X & u_Y & u_Z \end{bmatrix}^T$ the non-dimensional control vector expressed in the inertial frame. The constraints involved in the OCP formulation consist into three-point boundary conditions (an initial, a final and an intermediate boundary condition relative to the initial guess patching point) and a path constraint relative to the non-dimensional control vector. The initial boundary condition is

$$\boldsymbol{\psi}_0 = \boldsymbol{\psi}\left(\boldsymbol{y}(t_0), \boldsymbol{u}(t_0), \boldsymbol{p}, t_0\right) = \begin{Bmatrix} \boldsymbol{R}(t_0) - \boldsymbol{R}_0 \\ \boldsymbol{V}(t_0) - \boldsymbol{V}_0 \end{Bmatrix} = \boldsymbol{0} \tag{8}$$

where $\boldsymbol{R}_0$ and $\boldsymbol{V}_0$ are respectively the initial values for the position and velocity vector, assumed at the beginning of the by the initial guess arc considered.

In a similar way, the final boundary condition is defined by

$$\boldsymbol{\psi}_f = \boldsymbol{\psi}\left(\boldsymbol{y}(t_f), \boldsymbol{u}(t_f), \boldsymbol{p}, t_f\right) = \begin{Bmatrix} \boldsymbol{R}(t_f) - \boldsymbol{R}_f \\ \boldsymbol{V}(t_f) - \boldsymbol{V}_f \end{Bmatrix} = \boldsymbol{0} \tag{9}$$

where $\boldsymbol{R}_f$ and $\boldsymbol{V}_f$ are respectively the final values for the position and velocity vector, assumed at the end of the by the initial guess arc considered. The third and last boundary condition is related to the initial guess patching point, in which an impulsive Δv is applied. The condition states that, for a low-thrust trajectory, both the position and velocity vectors – although free to vary – must match across the patching point and thus no impulsive change in velocity is allowed:

$$\boldsymbol{\psi}_p = \boldsymbol{\psi}\left(\boldsymbol{y}(t_p), \boldsymbol{u}(t_p), \boldsymbol{p}, t_p\right) = \begin{Bmatrix} t_p^+ - t_p^- \\ \boldsymbol{R}(t_p^+) - \boldsymbol{R}(t_p^-) \\ \boldsymbol{V}(t_p^+) - \boldsymbol{V}(t_p^-) \end{Bmatrix} = \boldsymbol{0} \tag{10}$$

As shown in (10), a time continuity condition (across the patching point) has to be also imposed for a correct formulation of the optimal control problem. Finally, the path constraint consists in the nonlinear inequality condition on the non-dimensional control, stated below in (11):

$$\left\|\boldsymbol{u}(t)\right\| \leq 1 \tag{11}$$

This condition allows the control acceleration to vary, in every point of the transfer, only between 0 and $a_{\max}$. It is worth to note that the OCP thus formulated consists into a multiple-phase OCP where, in the specific, two phases are involved and coincident respectively with the first trajectory arc before the patching point and the second one, after the patching point.

The final OCP, with variable spacecraft mass and referred as $\mathcal{P}_2$, slightly differs from $\mathcal{P}_1$ in the dynamics, since the mass variation equation has to be considered

$$\dot{\boldsymbol{y}} = \boldsymbol{f}\left(\boldsymbol{y}(t), \boldsymbol{u}(t), \boldsymbol{p}, t\right) \tag{12}$$

$$= \begin{cases} \dot{\boldsymbol{R}} = \boldsymbol{V} \\ \dot{\boldsymbol{V}} = -\mu_{\odot}\dfrac{\boldsymbol{R}}{\left\|\boldsymbol{R}\right\|^3} - \mu_{\oplus}\dfrac{\left(\boldsymbol{R}-\boldsymbol{R}_{\oplus}\right)}{\left\|\boldsymbol{R}-\boldsymbol{R}_{\oplus}\right\|^3} - \mu_{M}\dfrac{\left(\boldsymbol{R}-\boldsymbol{R}_{M}\right)}{\left\|\boldsymbol{R}-\boldsymbol{R}_{M}\right\|^3} + \dfrac{T_{\max}}{m}\boldsymbol{u} \\ \dot{m} = -\dfrac{T_{\max}}{{}^{(LT)}I_{sp}\, g_0}\left\|\boldsymbol{u}\right\| \end{cases}$$

and in the following boundary conditions, where the matching condition on the mass has also to be included:

$$\boldsymbol{\psi}_0 = \boldsymbol{\psi}\left(\boldsymbol{y}(t_0), \boldsymbol{u}(t_0), \boldsymbol{p}, t_0\right) = \begin{Bmatrix} \boldsymbol{R}(t_0) - \boldsymbol{R}_0 \\ \boldsymbol{V}(t_0) - \boldsymbol{V}_0 \\ m(t_0) - m_0 \end{Bmatrix} = \boldsymbol{0} \tag{13}$$

$$\boldsymbol{\psi}_p = \boldsymbol{\psi}\left(\boldsymbol{y}(t_p), \boldsymbol{u}(t_p), \boldsymbol{p}, t_p\right) = \begin{Bmatrix} t_p^+ - t_p^- \\ \boldsymbol{R}(t_p^+) - \boldsymbol{R}(t_p^-) \\ \boldsymbol{V}(t_p^+) - \boldsymbol{V}(t_p^-) \\ m(t_p^+) - m(t_p^-) \end{Bmatrix} = \boldsymbol{0} \tag{14}$$

In (12) m is the spacecraft's mass, $T_{\max}$ the maximum thrust that can be provided by the low-thrust system, ${}^{(LT)}I_{sp}$ the low-thrust specific impulse and g_0 the standard gravitational acceleration. In (13), m_0 indicates the value of the spacecraft's mass at the beginning of the 4-body transfer.

It shall be noted that during the continuation process employed to achieve the final optimal transfer solution, the optimiser may converge into local minima characterised by a time of flight higher than the initial guess one. Since optimal solutions in terms of low Δv (or fuel mass consumption, in the case of mass variation) are desirable, with a transfer time as short as possible, an artifice has been adopted to lead the continuation process to a final acceptable optimal solution. The expedient consists in starting the continuation from the solution of a minimum time of flight OCP and then carrying on the iterative process by solving the $\mathcal{P}_1$ OCP. The minimum transfer time optimal control problem, here defined as $\mathcal{P}_3$, is identical to $\mathcal{P}_1$ except in the objective function, that is:

$$J = t_{0f} = t_f - t_0 \tag{15}$$

IV.II. Escape trajectory from the Earth

The escape transfer from the Earth takes place from the perigee of a GTO, with perigee altitude $h_p = 200$ km. The GTO is coplanar with the target orbit of the escape trajectory, which is the osculating orbit relative to the Earth closest approaching point of the Earth-Moon transfer. Both the orbits lie on the ecliptic's plane. Furthermore, it is assumed that the argument of the perigee of the GTO is the same of the target orbit.

Regarding the purely low-thrust escape transfer from the Earth, a preliminary framework has been set up before solving the trajectory optimisation problem. In fact, for the specific transfer problems at hand, low-thrust transfers involve a large number of revolutions, of the order of hundreds. Traditional trajectory optimisation methods, based on direct or indirect approaches, would generally require a high computational effort and are usually hard to solve numerically. For the purpose of a first analysis study carried out in the current work, a simplified optimal control law has been adopted for the low-thrust transfer; furthermore, the dynamics considered in the OCP formulation is the one relative to a 2-body model.

Specifically, Gao's steering law was adopted to compute the low-thrust transfer.[11,12] The parameters involved in the steering-law formulation have been optimally tuned in order to obtain a feasible transfer solution and minimising, at the same time, a selected cost function. The minimum time of flight cost function has been selected, as previously explained and motivated at the beginning of this section. The optimisation has been performed by using a

Particle Swarm Optimisation (PSO) solver*, which has proven to be effective in the heuristic solution of the optimal problem at hand. The OCP with Gao's steering law (defined as $\mathcal{P}_G$) consists in the problem to find the optimal values of $\boldsymbol{\lambda} = \begin{bmatrix} p_s & p_e & f_{in} & t_{0f} \end{bmatrix}$ to minimise the cost function (15), subjected to the 2-body dynamics equations (formulated in Keplerian coordinates and in an Earth-centred inertial reference frame, with the same orientation in the space of the Sun-centred inertial)

$$\dot{\boldsymbol{y}} = \boldsymbol{f}\left(\boldsymbol{y}(t), \boldsymbol{u}(t), \boldsymbol{p}, t\right) \tag{16}$$

$$= \begin{cases} \dot{a} = \dfrac{2a^2 e \sin(\vartheta)}{h} u_r + \dfrac{2a^2 p}{hr} u_\vartheta \\ \dot{e} = \dfrac{1}{h} p \sin(\vartheta) u_r + \dfrac{1}{h}\left[(p+r)\cos(\vartheta) + re\right] u_\vartheta \\ \dot{i} = \dfrac{r\cos(\omega+\vartheta)}{h} u_h \\ \dot{\Omega} = \dfrac{r\sin(\omega+\vartheta)}{h\sin(i)} u_h \\ \dot{\omega} = -\dfrac{p\cos(\vartheta)}{he} u_r + \dfrac{(p+r)\sin(\vartheta)}{he} u_\vartheta \\ \qquad -\dfrac{r\sin(\omega+\vartheta)\cos(i)}{h\sin(i)} u_h \\ \dot{\vartheta} = \dfrac{h}{r^2} - \dot{\omega} - \dot{\Omega}\cos(i) \\ \dot{m} = -\dfrac{T_{\max}}{(LT) I_{sp} g_0} \|\boldsymbol{u}\| \end{cases}$$

with $p = a\left(1-e^2\right)$, $h = \sqrt{\mu_\oplus p}$, $r = p/\left(1+e\cos(\vartheta)\right)$,

the Gao's steering-law

$$\begin{aligned} &\underbrace{\text{tangential}}_{-\pi p_s \le \vartheta \le \pi p_s} \quad \begin{cases} \boldsymbol{u} = \text{sign}(p_s) f_{in} \dfrac{T_{\max}}{m} \dfrac{{}^{(r,\vartheta,h)}\boldsymbol{V}}{\left\| {}^{(r,\vartheta,h)}\boldsymbol{V} \right\|} \end{cases} \\ &\underbrace{\text{inertial}}_{\pi(1-p_e) \le \vartheta \le \pi(1+p_e)} \quad \begin{cases} \boldsymbol{u} = \text{sign}(p_e) f_{in} \dfrac{T_{\max}}{m} \begin{bmatrix} \sin(\vartheta) \\ \cos(\vartheta) \\ 0 \end{bmatrix} \end{cases} \end{aligned} \tag{17}$$

with $-1 \le p_s \le 1$, $-1 \le p_e \le 1$, $0 \le f_{in} \le 1$

and the two following constraints, respectively on the control and the final state

$$\psi_c = |p_s| + |p_e| - 1 \le 0 \tag{18}$$

$$\psi_f = \left[\left(a(t_f) - a_f\right)^2 + \left(e(t_f) - e_f\right)^2 + \left(i(t_f) - i_f\right)^2 + \left(\Omega(t_f) - \Omega_f\right)^2 + \left(\omega(t_f) - \omega_f\right)^2 \right]^{0.5} \le \varepsilon = 10^{-2} \tag{19}$$

The parameters p_s and p_e define the amplitude of the thrust arcs relative to the tangential and inertial steering law and respectively around the perigee and apogee; f_{in} is the non-dimensional magnitude of the control. In (16) and (17) the control vector $\boldsymbol{u} = \begin{bmatrix} u_r & u_\vartheta & u_h \end{bmatrix}^T$ is expressed in the (r, ϑ, h) frame, i.e. the orbital frame, centred in the spacecraft, with r-axis having the same direction and versus of the Cartesian position vector, h-axis with direction and versus of the orbital angular momentum and ϑ-axis pointing in the versus of the orbital velocity. In (17) ${}^{(r,\vartheta,h)}\boldsymbol{V}$ represents the Cartesian velocity vector also expressed in the (r, ϑ, h) frame. Finally, the constraint condition in (18) states that the two steering laws – tangential and inertial – cannot overlap; the condition in (19) is necessary in order to enforce the boundary condition on the final state of the escape transfer, which must only match the first five components $\begin{bmatrix} a_f & e_f & i_f & \Omega_f & \omega_f \end{bmatrix}$ of the state of the target orbit, within a pre-set tolerance ε. It should be noted that, in this way, only an orbit transfer to the target orbit is guaranteed, instead of a rendezvous with the starting point of the main Earth-Moon transfer. This has been necessary in order to improve the convergence of the heuristic solver, which otherwise would have hardly converged to a feasible solution. In order to reach the Earth closest approaching point, a coasting arc takes place, after the orbit transfer, to the position of this point on the target orbit.

Regarding the only high-thrust escape trajectory from the Earth, a simple Hohmann transfer solution has been employed, followed by a coasting arc for injecting into the 4-body transfer to the Moon.

V. RESULTS

In the current section results for both low and hybrid-thrust optimal Earth-Moon transfers are shown and next discussed. These solutions represent a set of trade-off options – between the time of flight and the fuel consumption – for a more convenient selection of an Earth-Moon transfer, according to specific mission requirements. In fact, due to particular demands, the choice of a solution respect to another can be determined by the necessity to save more fuel mass but taking a longer time to complete the transfer or, conversely, spending a shorter time for the transfer but consuming more fuel. Low and hybrid-thrust optimal transfers have been computed for each initial guess

*PPSO solver retrieved on 29th August 2016 at: https://uk.mathworks.com/matlabcentral/fileexchange/58895-ppso.

solution, for a total of 6 optimal Earth-Moon transfer options organised in 2 sets, each one for each propulsion option considered (i.e. low and hybrid-thrust). For each set, only the best results, in terms of fuel mass consumption (and time of flight), are illustrated. A full summary of the results for all the transfer options computed is instead provided in Table 2 and Table 3., respectively for low and hybrid-thrust transfers. Before illustrating the results, numerical values need to be specified for the parameters related to the propulsion systems employed. Specifically, the maximum thrust has been set to $T_{\max} = 0.3$ N, except in the case of the 4-body transfer relative to the IG3 solution where $T_{\max} = 0.5$ N (because no further solutions, with a lower value of the maximum thrust, were possible to be computed by means of the continuation process). The low-thrust specific impulse has been set to ${}^{(LT)}I_{sp} = 3000$ s, while the high-thrust specific impulse is ${}^{(HT)}I_{sp} = 300$ s. The value of the spacecraft's mass at the departure from the GTO orbit has been set to 1000 kg and the spacecraft's dry mass to $m_{dry} = 500$ kg.

IG1: low-thrust transfer

In Figure 7 the best found full low-thrust optimal Earth-Moon transfer is represented. The profile over time of the control thrust components is shown in Figure 8 and Figure 9, respectively for the escape transfer from the Earth and the main Earth-Moon transfer.

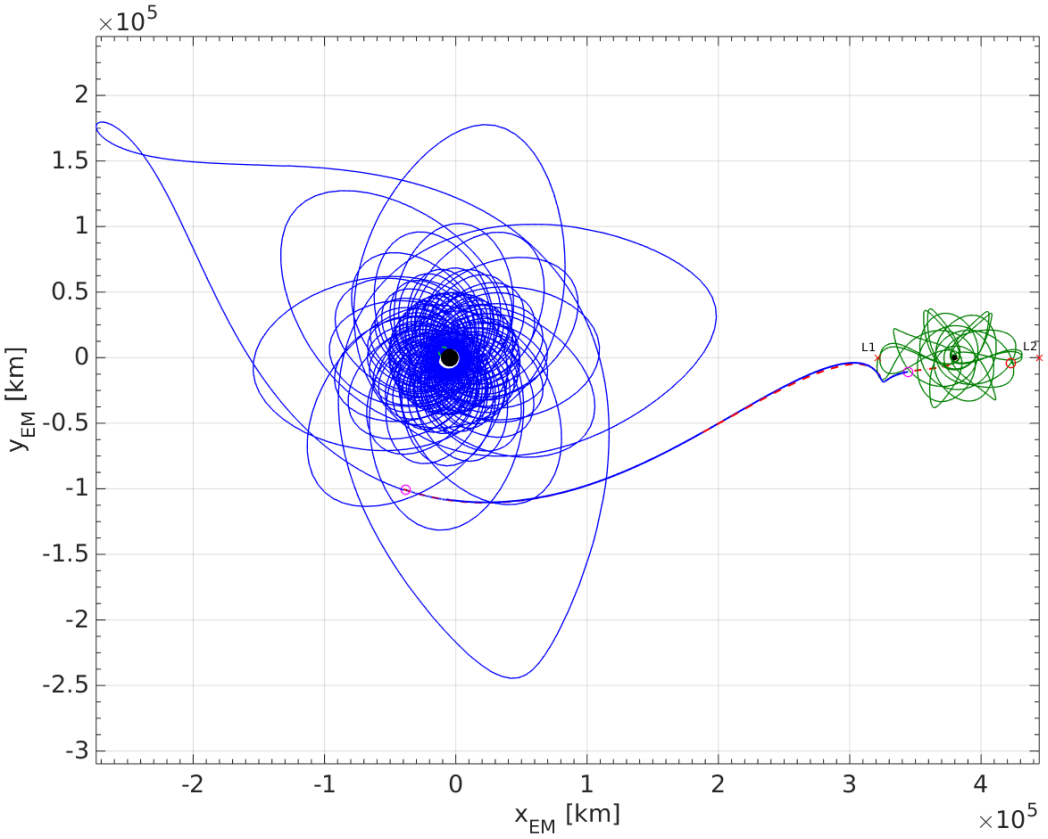

Figure 7. Optimal low-thrust Earth-Moon transfer based on IG1. The red dotted line represents the initial guess solution in the coupled-CR3BP and the thick blue line the respective optimal solution in the BCR4BP. The blue line trajectory injecting in the optimal 4-body transfer consists in the escape transfer from the Earth. The green line trajectory at the end of the 4-body transfer represents the capture trajectory around the Moon.

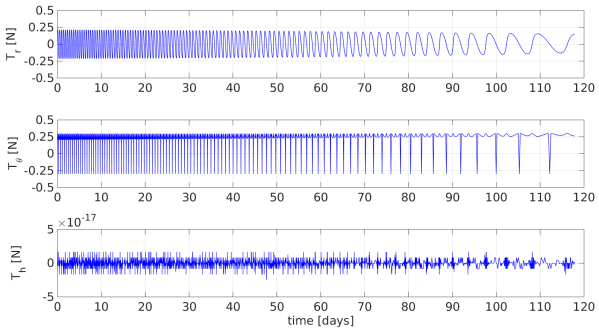

Figure 8. Thrust components in the orbital frame as function of time for the low-thrust escape trajectory from the Earth (T_{max} = 0.3 N). Note that the final time corresponds to the time of flight for the rendezvous with the osculating orbit relative to the Earth closest approaching point of the 4-body transfer.

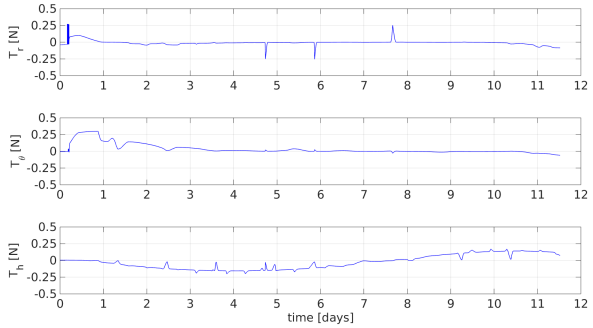

Figure 9. Thrust components in the orbital frame as function of time for the low-thrust 4-body transfer to the Moon (T_{max} = 0.3 N). Note that the time has been reset to 0 at the starting point of the 4-body transfer.

In Figure 10 and Figure 11 the spacecraft's mass profile over time is shown, respectively for the escape transfer from the Earth and the main Earth-Moon transfer.

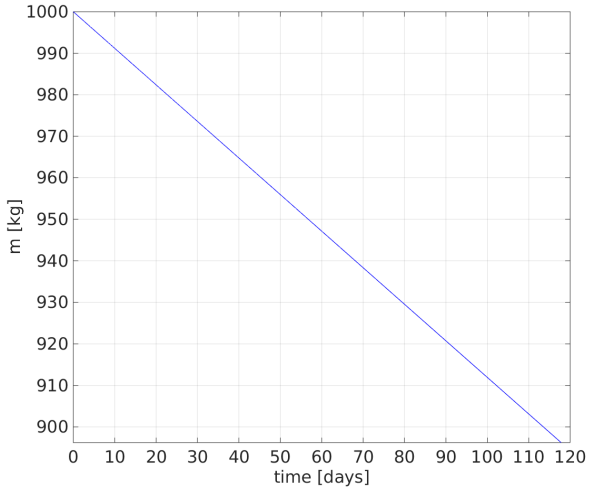

Figure 10. Spacecraft mass profile over time for the low-thrust escape trajectory from the Earth.

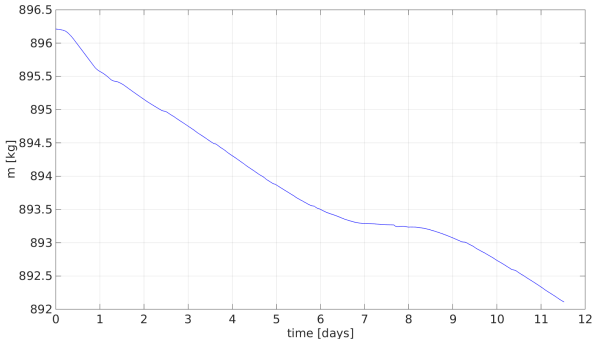

Figure 11. Spacecraft mass profile over time for the low-thrust 4-body transfer to the Moon.

IG3: hybrid-thrust transfer

In Figure 12 the best hybrid-thrust optimal Earth-Moon transfer is represented. The profile over time of the control thrust components and the spacecraft's mass is shown respectively in Figure 13 and Figure 14, for the main Earth-Moon transfer trajectory. The values of the fuel mass consumption, relative to the two impulsive manoeuvres in the escape transfer from the Earth, are shown in Table 3.

Results summary

A full summary of the results, for all the computed optimal Earth-Moon transfer solutions, is below provided in Table 2 and Table 3. Here Δm_I, $t_{0f,I}$ and Δm_{II}, $t_{0f,II}$ are the fuel mass consumption and time of flight, respectively for the escape transfer from the Earth and the main Earth-Moon transfer.

Table 2. Summary of results in terms of fuel mass consumption and time of flight for the low-thrust Earth-Moon transfers.

IG #	T_{max} [N]	Δm		t_{0f}	
		Δm_I [kg]	Δm_{II} [kg]	$t_{0f,I}$ [days]	$t_{0f,II}$ [days]
1	0.3	107.9		139.23	
		103.8	4.1	127.71	11.52
2	0.3	118.2		146.22	
		110.9	7.3	134.99	11.23
3	0.5	127.4		141.04	
		114.4	13	129.93	11.11

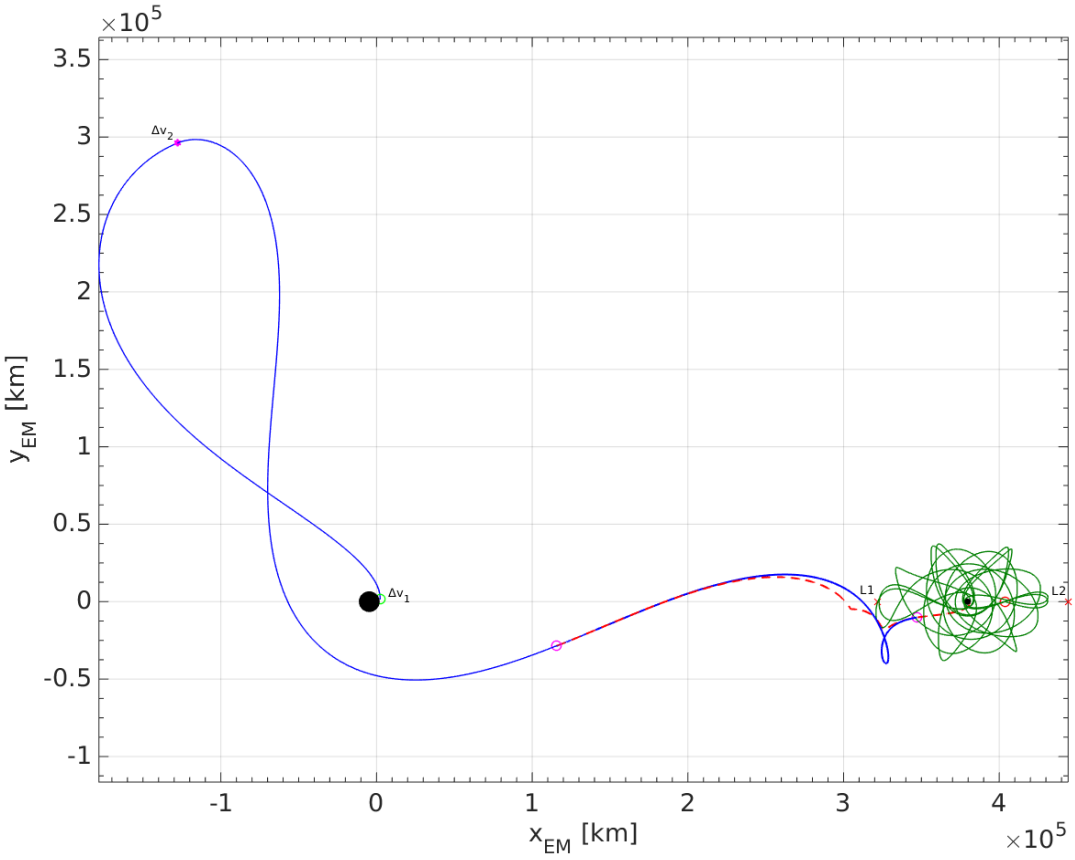

Figure 12. Optimal hybrid-thrust Earth-Moon transfer based on the IG3 starting solution. The red dotted line represents the initial guess solution in the coupled-CR3BP and the thick blue line the respective optimal solution in the BCR4BP. The blue line trajectory injecting in the optimal 4-body transfer consists in the high-thrust escape transfer from the Earth. The green line trajectory at the end of the 4-body transfer represents the capture trajectory around the Moon. The two Δv of the high-thrust transfer are respectively Δv_1 = 665.89 m/s and Δv_2 = 555.62 m/s.

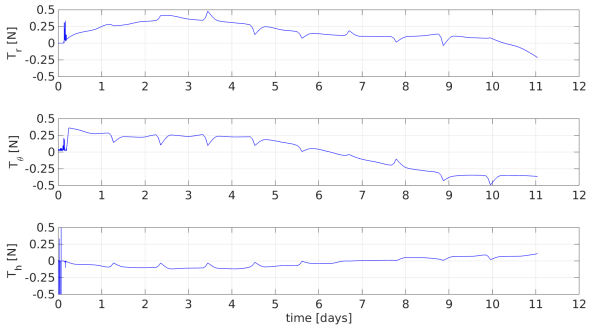

Figure 13. Thrust components in the orbital frame as function of time for the low-thrust 4-body transfer to the Moon (T_{max} = 0.5 N). Note that the time has been reset to 0 at the starting point of the 4-body transfer.

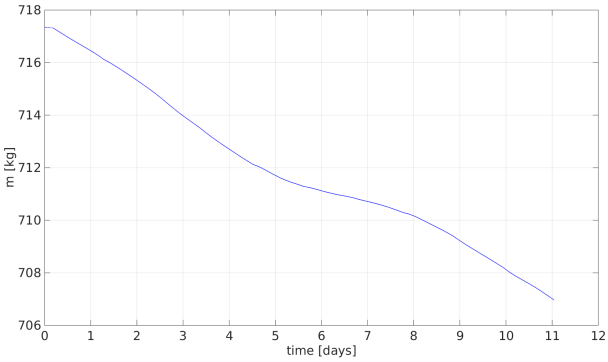

Figure 14. Spacecraft mass profile over time for the low-thrust 4-body transfer to the Moon.

Table 3. Summary of results in terms of fuel mass consumption and time of flight for the hybrid-thrust Earth-Moon transfers.

IG #	$T_{\max}$ [N]	Δm		t_{0f}	
		Δm_I [kg]	Δm_{II} [kg]	$t_{0f,I}$ [days]	$t_{0f,II}$ [days]
1	0.3	343.0		20.80	
		339.8	3.2	9.61	11.19
2	0.3	314.2		19.75	
		308.6	5.6	8.96	10.79
3	0.5	293.0		19.95	
		282.7	10.3	8.91	11.04

As it is possible to see from the results presented above, the best solution in terms of fuel mass consumption for a low-thrust only transfer is the one relative to IG1. This solution also exhibits the lower time of flight among the three transfer options in Table 2. The best solution computed for a hybrid-thrust transfer to the Moon is instead the one relative to IG3, which exhibits the lowest consumption in terms of fuel mass among the three options in Table 3. This hybrid-thrust solution is characterised by a time of flight around 8.7 times lower the one of the best low-thrust solution mentioned above. However, the fuel mass consumption is around 2.6 times higher, but still far below the fuel budget assigned for the mission.

Comparison with optimal high-thrust transfers

The optimal low and hybrid-thrust solutions found in the current work are here compared with optimal high-thrust Earth-Moon transfers in the 4-body dynamics, retrieved in literature from [13]. Specifically, in the referenced paper families of optimal two-impulse Earth-Moon transfers are obtained in the planar bicircular restricted four body dynamics. These solutions are grouped into families, according to their distinctive characteristics. The optimal impulsive transfers are bounded in terms of time of flight t_{0f} and Δv as follows:

$$\begin{aligned} 3.75 \le \Delta v \le 4.15 \ \text{km/s} \\ 5 \le t_{0f} \le 100 \ \text{days} \end{aligned} \quad (20)$$

The initial and final boundary conditions for the impulsive transfers consist into a departing circular orbit from the Earth – with altitude of $h_i = 167\,\text{km}$ – and into an arriving circular orbit at the Moon with altitude $h_f = 100\,\text{km}$. It has to be noted that only a subset of these solutions (characterised by a time of flight higher than 60 days) end into a ballistic capture around the Moon. At this point an important remark is to be made: as already discussed, all the solutions computed in this work inject into a ballistic capture around the Moon (lasting almost 6 months), after passing by the perilune at an altitude h_{MCAP} (comparable to h_f). However, they do not necessarily get into a circular Moon orbit after reaching the perilune. Therefore, due to different arriving conditions around the Moon, a completely fair and accurate comparison cannot be done between the high-thrust solutions of [13] and the low and hybrid-thrust ones presented in this paper. However, the considerations explained below have been adopted in order to have an idea of the order of magnitude for the Δv-cost of the impulsive trajectories, referred to a transfer scenario the as close as possible to the one adopted in the current work.

An initial impulsive Δv has been calculated in order to convert the departing circular orbit of altitude h_i to a GTO orbit with perigee altitude equal to h_i. Because of a comparable altitude at the perigee, the GTO orbit thus obtained can be compared with the departing GTO orbit of the optimal transfers computed in the current work (see section IV.II). The impulsive Δv required is $\Delta v_i = 2.46\,\text{km/s}$. This latter value has been subtracted to both the boundary Δv values in (20), thus giving:

$$1.29 \le \Delta v' \le 1.69 \ \text{km/s} \quad (21)$$

The boundary values in (21) define, in a first approximation, the range of the cost values – in terms of Δv – of the optimal high-thrust Earth-Moon transfers, if compared to the optimal low and hybrid thrust solutions presented in this paper. By making use of the Tsiolkovsky equation, a value can be computed for the minimum fuel mass consumption required by the impulsive transfers. In fact, by considering $\Delta v'_{\min} = 1.29\,\text{km/s}$, it results:

$$\Delta m_{HT,\min} = m_0 \left(1 - e^{-\frac{\Delta v'_{\min}}{(HT) I_{sp} g_0}} \right) = 354.89\,\text{kg} \quad (22)$$

where $\Delta m_{HT,\min}$ is the minimum fuel mass required by the high-thrust transfers in [13]. This value is in line with the values of fuel mass consumption in Table 3, which are the highest ones obtained for the optimal transfer solutions computed in the current work. Furthermore, it has to be noted that the high-thrust solutions in [13] with a lower Δv cost are characterised by a time of flight higher than 70 days. Conversely, the solutions in Table 3 exhibit a transfer time of about 20 days, which is more than 3 times lower than the one of the impulsive solutions with lowest Δv.

VI. CONCLUSIONS

The work carried out and presented in this paper has produced, as a final result, sets of optimal low and hybrid-thrust Earth-Moon trajectories that constitute trade-off options between Δv (or, equivalently, fuel mass consumption) and time of flight. Optimal high-thrust trajectories have been retrieved from literature and taken into account, in order to complete the sets of possible options for the Earth-Moon transfers. The optimal high, low and hybrid-thrust trajectories have been compared between each other, so that the advantages and the drawbacks of each transfer option could be highlighted. Specifically, fully low-thrust transfers exhibit the lowest fuel mass consumption (about 110 kg in the best case), despite of a higher time of flight (around 140 days), but still constrained within an admissible transfer duration. On another hand, hybrid-thrust solutions require a fuel consumption up to almost 3 times higher than the one of low-thrust transfers, but with the important benefit of a time of flight around 9 times lower. Finally, the fully high-thrust Earth-Moon transfer solutions retrieved from literature show that, in the best case and in a first approximation, these trajectories have a fuel mass consumption comparable with the one of hybrid-thrust transfers but with a respective time of flight about 3 times higher than the one of the same hybrid-thrust solutions. However, faster solutions are available with only high-thrust propulsion and down to 5 days of transfer time, but with the drawback of the highest fuel mass consumption among all the solutions shown in this paper.

Future developments of the current work will essentially regard three main improvements to be carried out. The first consists in obtaining fully 4-body optimal solutions for the Earth-Moon transfers, including the escape trajectory form the Earth (which has been computed with the 2-body dynamics approximation in the current work). A second improvement is to develop a strategy able to consider together, in the optimisation process, both the optimal control problems relative to the escape trajectory from the Earth and the main Earth-Moon transfer. This is required in order to compute a more comprehensive optimal transfer solution, which could possibly be more advantageous than a sub-optimal patched solution, consisting in combining together two optimal transfers (as done in this paper). Finally, a full optimisation of the escape transfer from the Earth (by means, for example, of a direct transcription method) could be desirable, in order to possibly improve the optimality of the transfer solutions already computed.

VII. REFERENCES

1. Crawford, I. A., "Lunar resources: A review," *Progress in Physical Geography*, vol. 39, 2015, pp. 137–167.
2. Hubbard, S., "What Do We Do with the Moon?," *New Space*, vol. 4, 2016, pp. 1–1.
3. Price, H., Baker, J., and Naderi, F., "A Minimal Architecture for Human Journeys to Mars," *New Space*, vol. 3, 2015, pp. 73–81.
4. Sousa-Silva, P. A., O. Terra, M., and Ceriotti, M., "Novel fast low-cost Earth-Moon transfers with patched three-body systems," *Celestial Mechanics and Dynamical Astronomy (under revision)*.
5. Sousa-Silva, P. A., O. Terra, M., McInnes, C. R., and Ceriotti, M., "A heuristic strategy to compute ensembles of trajectories for 3D low-cost Earth-Moon transfers," *67th International Astronautical Congress*, 2016.
6. Curtis, H. D., *Orbital Mechanics for Engineering Students (Third Edition)*, 2014.
7. Koon, W. S., Lo, M. W., Marsden, J. E., and Ross, S. D., *Dynamical systems, the three-body problem and space mission design*, 2008.
8. Patterson, M. A., and Rao, A. V., "GPOPS-II: A MATLAB Software for Solving Multiple-Phase Optimal Control Problems Using hp-Adaptive Gaussian Quadrature Collocation Methods and Sparse Nonlinear Programming," *ACM Transactions on Mathematical Software*, 2013.
9. Gill, P. E., Murray, W., and Saunders, M. A., "SNOPT: An SQP Algorithm for Large-Scale Constrained Optimization," *SIAM Journal on Optimization*, vol. 12, 2002, pp. 979–1006.
10. Weinstein, M. J., and Rao, A. V., "A Source Transformation via Operator Overloading Method for the Automatic Differentiation of Mathematical Functions in MATLAB," *ACM Transactions on Mathematical Software*, 2014.
11. Gao, Y., "Near-Optimal Very Low-Thrust Earth-Orbit Transfers and Guidance Schemes," *Journal of Guidance, Control, and Dynamics*, vol. 30, 2007, pp. 529–539.
12. Heiligers, J., Ceriotti, M., Mcinnes, C. R., and Biggs, J. D., "Design of optimal Earth pole-sitter transfers using low-thrust propulsion," *Acta Astronautica*, vol. 79, 2012, pp. 253–268.
13. Topputo, F., "On optimal two-impulse Earth-Moon transfers in a four-body model," *Celestial Mechanics and Dynamical Astronomy*, vol. 117, 2013, pp. 279–313.